Full Paper Transactions, SMiRT 28
Toronto, Canada, August 10-15, 2025

Experimental Investigation into the Dynamic Response of a CANDU Fuel Bundle Endplate

Ali Saudy[1], Atef Mohany[2], Marwan Hassan[3], and Ross Lewis[3]

[1] PhD Student, Ontario Tech University, Oshawa, ON, Canada (ali.saudy@ontariotechu.net)
[2] Professor, Ontario Tech University, Oshawa, ON, Canada (atef.mohany@ontariotechu.ca)
[3] Professor, University of Guelph, Guelph, ON, Canada (mahassan@uoguelph.ca)
[4] Fuel Design Engineer, Bruce Power, Tiverton, ON, Canada (ross.lewis@brucepower.com)

ABSTRACT

This paper discusses the experimental investigation of the vibration response of the endplate in a CANDU 37M fuel bundle. The endplate's complex structural geometry results in a complex dynamic response characterized by multiple vibration frequencies. The contact dynamics between the fuel bundle and the pressure tube are replicated using a high precision custom-made experimental setup. Additionally, the contact between the fuel bundle and the neighbouring fuel bundles are replicated using dummy endplates. Multiple laser sensors were utilized simultaneously to accurately capture the phase shift and mode shapes of the endplate as it is excited continuously by an electrodynamic shaker across a specified range of frequencies. This paper presents the displacement and frequency responses of the endplate at specific frequencies as well as the corresponding mode shapes and the frequency response functions.

INTRODUCTION

The endplate is one of the most vital components of the CANDU Fuel Bundle. The fuel bundle consists of 37 zirconium rods, called fuel elements, welded together at both ends to a zirconium "endplate" with a complex geometry. The geometry of the endplate accommodates one central fuel element, six elements on its inner ring, 12 elements on the intermediate ring, and 18 elements on the outer ring as shown in Figure 1.

In a single fuel channel within a CANDU reactor, there are 12 fuel bundles stacked horizontally to form a single fuel string. These fuel bundles are not fixed in place and are allowed to slide and rotate as the heavy water coolant flows through the channels. The coolant flows through the channels at a rate of approximately 32 kg/s, reaching velocities up to 10 m/s [1]. This high flow rate results in turbulent flow. Additionally, acoustic waves generated from the pressure pulsations of the primary heat transport pump propagate with the coolant. If the frequency of the acoustic pressure pulsations matches one of the natural frequencies of the fuel bundle, it can lead to excessive vibration, potentially compromising the structural integrity of the bundle [2] [3]. Therefore, investigating the mode shapes and the phase shift of the endplate is of paramount importance. This paper presents an experimental modal analysis conducted to investigate the natural frequencies and mode shapes of the CANDU fuel bundle's endplate.

EXPERIMENTAL SETUP

A mock-up CANDU fuel bundle was obtained from its official manufacturers, Cameco Fuel Manufacturing (CFM). Instead of the standard uranium dioxide (UO_2) pellets used in actual fuel element, this mock-up bundle contained molybdenum pellets. Molybdenum was selected due to its equivalent density to UO_2, ensuring that the mock-up bundle replicated the actual fuel bundle. In order to replicate the contact dynamics experienced by the fuel elements under in-reactor conditions, a custom-made high precision experimental setup was developed. This setup was specifically engineered to support the mock-up bundle

during vibration testing while allowing for the non-intrusive measurement of its vibration characteristics. The design ensured accurate simulation of in-reactor conditions and provided the necessary accessibility for detailed vibration analysis.

Figure 1. CANDU 37M Bundle Endplate.

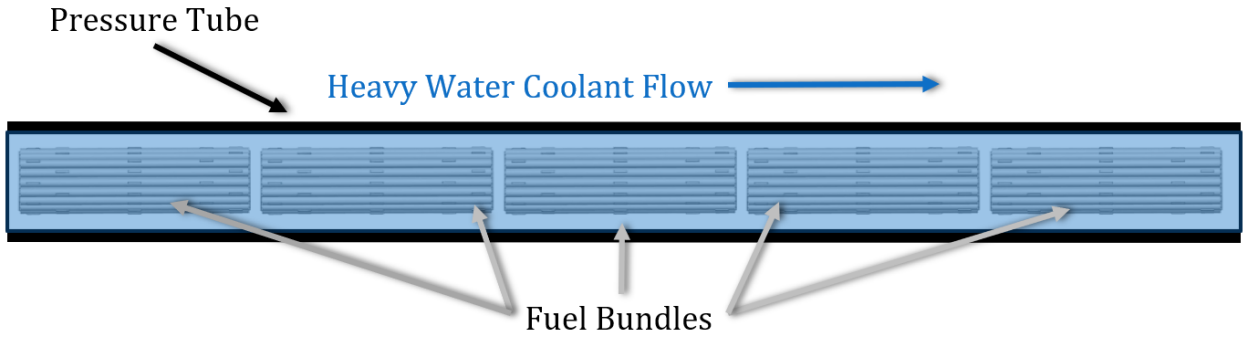

Figure 2. CANDU Pressure Tube Diagram.

The support assembly consists of a robust aluminium base plate, designed to allow five frames that support the bundle via its bearing pads. The fuel bundle contains beryllium brazed appendages on the exterior surface of the outer ring of fuel elements. These appendages create a radial clearance between the fuel

bundle and the surrounding pressure tube. The bundle includes five rings of bearing pads along the exterior fuel element. One ring of bearing pads positioned at the midspan of each element, while two additional rings are located near either end of the fuel element. The end rings are arranged in a staggered pattern from one fuel element to the next.

Each frame has a semi-circular cut matching the exact diameter of the pressure tube in the fuel channel. The frames were bolted in place on top of the aluminium base plate with high precision. It was essential that the five frames to be inline and level with one another so replicate the contact dynamics of the fuel bundle simulating the same behaviour as those in the actual fuel channel inside the reactor. The two frames at either ends of the bundle feature four threaded holes that surround the semi-circular cut to accommodate two aluminium dummy end plates. These endplates can be bolted onto either side of the support to mimic the presence of two neighbouring bundles in contact with the actual fuel bundle being tested. Each dummy plate has eight holes at 45° increments around the edge allowing the rotation in eight different angular orientations.

The endplate of the fuel bundle was assigned 84 different locations of measurement, divided into two classes:

- 37 locations corresponding to points where a fuel element is spot welded to the endplate
- 47 locations representing gaps between two adjacent fuel elements.

The 37 locations where a fuel element is spot welded, where 18 elements lie on the outer ring (similarly named OR1 to OR18), 12 elements lie on the intermediate ring (MR1 to MR12), six lie on the inner ring (IR1 to IR6), which surround one central element (C1). The 47 gaps that lie in between two adjacent fuel elements follow a similar pattern to the fuel element locations. There are 18 locations on the outer ring (O1 to O18), 12 locations on the intermediate ring (M1 to M12), six locations on the inner ring (I1 to I6), and then there are the web that connect the rings together, forming the physical geometry of the endplate. Each individual stem of the web was also deemed a location of interest for the measurement and they are donated as S1 to S11. These measurement locations are shown in Figure 3.

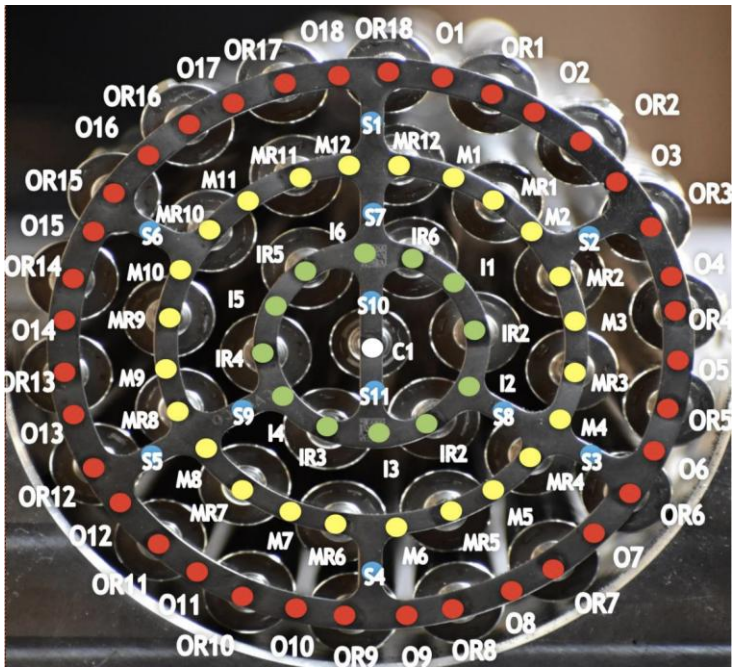

Figure 3. CANDU Fuel Bundle Endplate featuring the naming conventions of each point of measurement.

In these experiments, the endplate is subjected to a forced sinusoidal vibration using an electrodynamic shaker to perform a sine sweep across a range of frequencies between 10 Hz to 200 Hz. Both the shaker and the support assembly are bolted separately to the ground to eliminate cross-vibrations transmission. The sinusoidal force is applied by the shaker using a mechanism comprised of a threaded rod coming from the head of the shaker on which a force sensor is attached. The force sensor is then threaded into a specially designed clamp. The clamp can be fixed at any location in the endplate. Two pre-specified locations were identified on the endplate for excitation. During testing, it was noticed that exciting the top of the endplate produces the largest vibration amplitudes as the upper part of the fuel bundle is not in contact with the pressure tube. As a result, the shaker was attached to the bundle at two locations: O1 and M1. The shaker was exciting the endplate with a force of 30 N throughout the sine sweep. With the shaker attached to one end of the bundle, a dummy endplate could not be attached. As a result, a single dummy endplate was attached to the other side of the bundle.

Two laser sensors were utilized to measure the vibration of the endplate. One laser sensor was fixed at Location O2 serving as a reference point measurement, while the other laser sensor was utilized to measure each of the remaining 82 locations. The response of the two locations obtained simultaneously were compared to obtain the phase shift, and hence the mode shape can be determined. A display of the experimental setup is depicted in Figure 4.

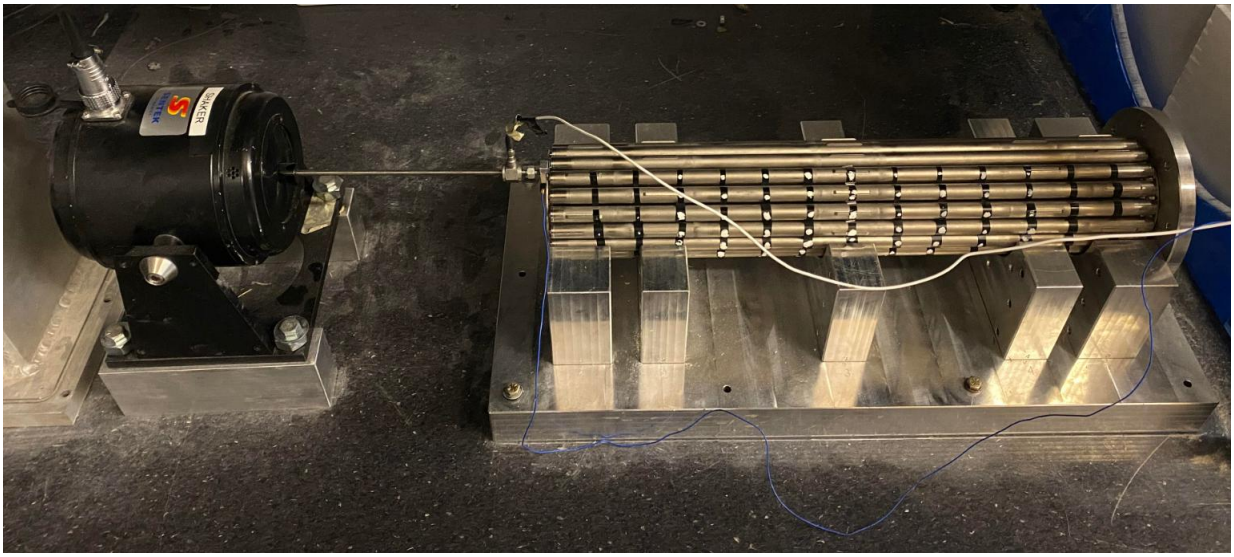

Figure 4. Experimental Setup for the vibration measurements.

DATA ANALYSIS

A custom MATLAB code was developed to automate the sine sweep process by controlling the signal sent to the power amplifier that drives the shaker. The frequency of the sinusoidal force induced by the shaker was held constant for 6 seconds before transitioning to the next frequency. The same code simultaneously recorded the displacement response over time from both laser sensors. The time-domain data were converted into the frequency domain via Fast Fourier Transform (FFT) enabling the identification of the dominant frequencies of each testing frequency. The dominant peak in the power vs. frequency graph was always the respective testing frequency in question. However, the amplitude of power would vary depending on the frequency. A maximum power curve or power spectrum was produced by creating a

function sweeping across the maximum power amplitude of each testing frequency. The highest power amplitudes indicate a resonant frequency of the endplate.

In this experiment, the phase shift between the displacement signals from the two points of measurements is calculated. Measurement at O2 is used as the reference point, and the other 82 locations of measurement across the endplate are the phase-relative points. A phase shift refers to the difference in phase between two periodic signals. It represents the time or angular difference between corresponding points (peaks or zero crossings) in two waveforms.

In this experiment, the phase shift between two signals provides insight into the dynamic behaviour of the endplate. A positive phase shift indicates that the displacement of the reference point O2 lags behind the other respective location being measured. In contrast, a negative phase shift indicates that the displacement of the reference point O2 leads the other measured location, meaning O2 reacts before the measured location. A phase shift of zero indicates synchronized motion, where the displacements at the two measured locations reach their peaks (or other corresponding points) simultaneously.

The phase shift is often frequency-dependent in mechanical systems. At certain frequencies (resonant frequencies for example), the phase shift may show significant changes, such as a shift from 0° to 180°, reflecting a change in the dynamics of the endplate. Since phase angles are periodic, the MATLAB script adjusts the calculated phase shift to lie within -180° and +180 for clarity and consistency.

RESULTS AND DISCUSSION

Figures 5a) and b) display the single-sided displacement spectra of all 82 points measured on the endplate during the sine sweep for when the shaker excited the endplate at O1 and M1. Figures 6a) and b) depict the phase shift plotted against each testing frequency for each of the 82 measured points during the sine sweep applied at O1 and M1 respectively. , Figures 7a) and b) display the deformation shape of the endplate in response to the two excitation points O1 and M1.

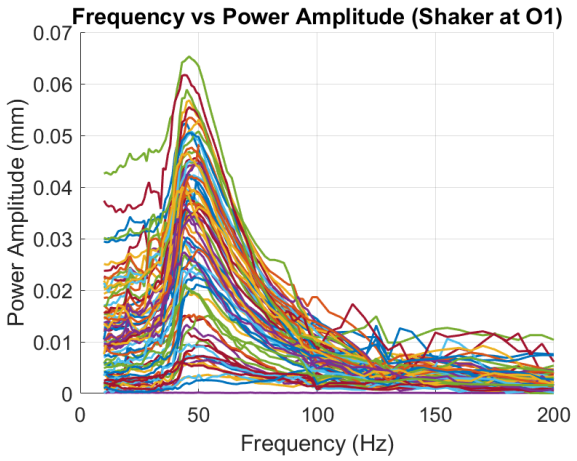

Figure 5a. Frequency response of the Endplate (Shaker at O1)

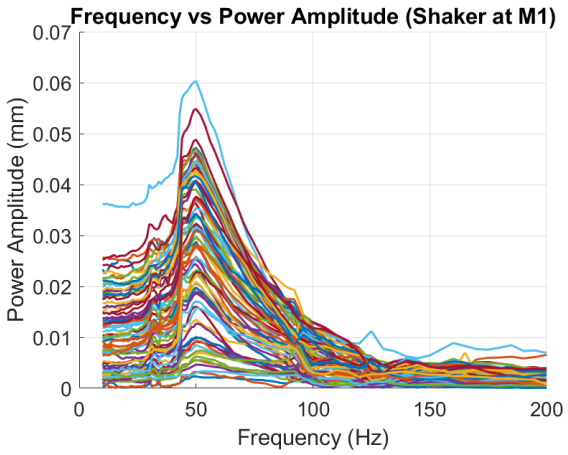

Figure 5b. Frequency response of the Endplate (Shaker at M1)

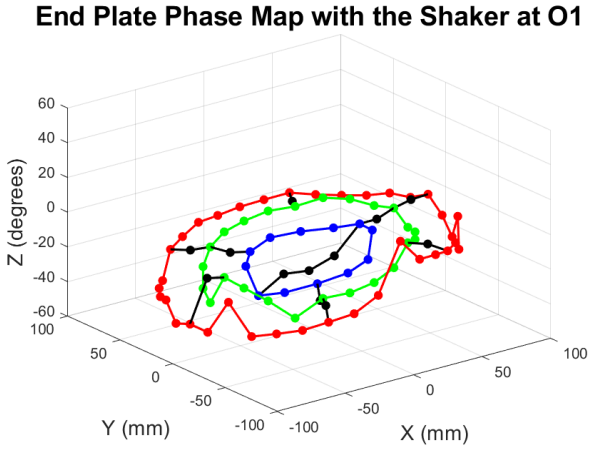

Figure 6a. Phase map of the Endplate at an excitation frequency of 50 Hz (Shaker at O1)

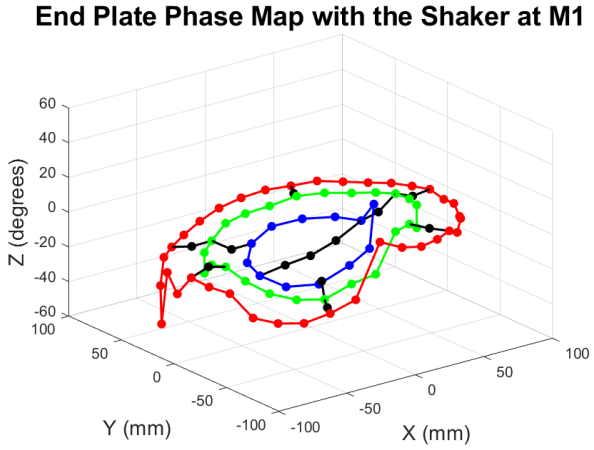

Figure 6b. Phase map of the Endplate at an excitation frequency of 50 Hz (Shaker at M1)

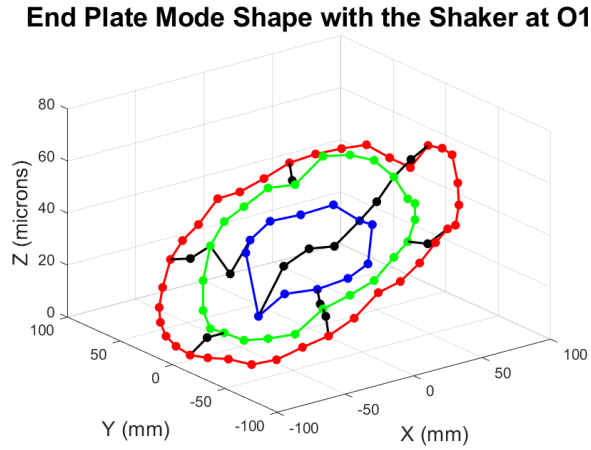

Figure 7a. Mode Shape of the Endplate at 50 Hz (Shaker at O1)

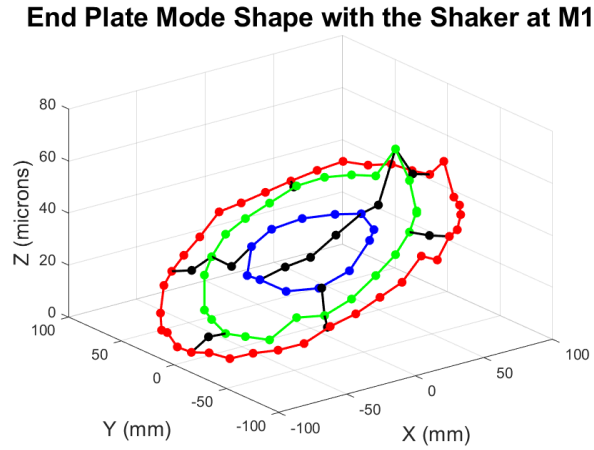

Figure 7b. Mode Shape of the Endplate at 50 Hz (Shaker at M1)

The endplate maximum deformation was observed at the topmost points of the outer and intermediate rings with displacements exceeding 60 μm in response to the 30 N excitation at O1. When the shaker is at M1 however, there is a noticeable drop in the amplitude of deformation at these locations, with displacements reaching up to a maximum of 50 μm. Therefore, it can be concluded that when the endplate is excited at relatively lower locations, it produces lower amplitudes of vibration. According to Figures 5a) and 5b), it can be clearly seen that there is a resonant frequency of the endplate at 50 Hz for all 82 measured locations on the endplate, in both cases. The initial spike can be seen around 35 Hz, which is already known to be the natural frequency of the attached fuel elements [4-5]. There are also peaks seen at around the 20 Hz range.

The phase shift between most of the measured locations of the endplate is generally consistent in the 50 Hz range, varying from -30° to +20°. In both cases, the lower points on the endplate demonstrated the largest variation in the phase (O8-O11). This is most likely due to the fact that the bearing pads in contact with the pressure tube at these locations, create a resistive friction force acting against the force induced from the shaker, allowing these points to experience a difference in phase.

Figures 6(a) and 6(b) depict the phase map across the structure of the endplate. The x and y coordinates indicate the physical point of each location of measurement, and the z coordinate indicate the positive or negative phase shift of each point compared to the reference point O2. The phase maps essentially indicate how different parts of the endplate vibrate relative to each other at the excitation frequency of 50 Hz. In the case where the shaker was at M1, the phase distribution appears slightly more uniform, suggesting a relatively symmetrical vibration response across the endplate. In the case where the shaker is at O1, the phase map shows a larger spread, particularly in the bottom half of the outer ring. This suggests that the location of the shaker at O1 introduces larger localized differences in the vibrational response. The phase across the entire endplate is generally synchronized. The tighter clustering of the phase angles in Figure 6(b) implies better phase synchronization when the shaker is positioned at M1. The phase variability in Figure 6(a) reflects that O1 might be closer to a nodal point or a location that induces asymmetry in the mode.

The overall mode shape of the endplate can be seen for both cases in Figures 7(a) and 7(b). It can clearly be seen that the points in the top half of the endplate vibrate with a greater amplitude than the lower half. As the height gradually decreases from the top of the bottom, so does the vibration amplitude at a fairly consistent rate. With the shaker at M1, the mode shape displayed localized peaks at points MR12 and O1, suggesting higher localized deformation. With the shaker at O1, the mode shape of the endplate exhibits asymmetry in the top half of the outer ring, suggesting that excitation at this point disrupts the symmetry of the system.

CONCLUSION

This paper summarizes the experimental procedure used to investigate the dynamic response of a CANDU fuel bundle endplate. A mock-up fuel bundle was acquired, and a specially designed, high precision experimental setup was manufactured to support the fuel bundle during the vibration tests, to ensure the precise contact dynamics of the fuel bundle sitting in the pressure tube are replicated in this experiment. An electrodynamic shaker applies a sine sweep to the endplate across a frequency range of 10 Hz to 200 Hz. The sine sweep was conducted at two locations: the top of the outer ring and the top of the intermediate ring. Two laser sensors were utilized to capture the displacement response. One sensor was held consistently at one location near the top of the outer ring, while the other laser sensor measures the other 82 required measurement locations.

The endplate demonstrates a similar frequency response when comparing the two cases. It can be deduced that exciting the endplate at a location in its upper half induces larger amplitudes of vibration across the endplate. Several points across the endplate reached vibration amplitudes of 60-70 μm in this case. Comparing this case to when the shaker was exciting the endplate at a lower location (the top of the intermediate ring), almost all points measured never exceeded vibration amplitudes more than 50 μm. The phase shift between the two cases shows generally consistent behaviour in the resonant frequency of 50 Hz. The position of the shaker plays a critical role in determining the vibrational behaviour of the endplate. When placed at O1, the excitation introduces localized effects and greater phase variability, indicating that O1 might be closer to a node or an area with low modal participation for this mode shape. When placed at M1, the excitation is more symmetric and produces a uniform vibrational response, likely because M1 is closer to the centre of mass or a point of high modal participation. These observations can guide future optimization techniques to ultimately mitigate fuel bundle vibration in the endplate.

ACKNOWLEDGEMENT

The authors would like to acknowledge the funding received by COG (CANDU Owners Group) and NSERC (Natural Sciences and Engineering Research Council of Canada) for the funding provided to carry out this work.

REFERENCES

[1] W. J. Garland, Ed., "The Essential CANDU - a textbook on the CANDU nuclear power plant technology,"CANDU textbook, 2014.

[2] Yetisir, M., and N.J. Fisher. "Prediction of Pressure Tube Fretting-Wear Damage due to Fuel Vibration." *Nuclear Engineering and Design*, vol. 176, no. 3, Nov. 1997, pp. 261–271.

[3] A. Mohany, and M. Hassan. "Modelling of Fuel Bundle Vibration and the Associated Fretting Wear in a CANDU Fuel Channel." *Nuclear Engineering and Design*, vol. 264, 1 Nov. 2013, pp. 214–222.

[4] O. Elbanhawy, A. Mohany, and M. Hassan, "Simulation of Motion-Dependent Fluid Forces in Fuel Bundles." *Nuclear Engineering and Design*, vol. 356, 4 Nov. 2019, pp. 110373.

[5] O. Elbanhawy, A. Mohany, and M. Hassan, "Modelling of Fully-Flexible Fuel Bundles." *Nuclear Engineering and Design*, vol. 378, July 2021, p. 111014.